Journal Of Chemistry And Material Sciences Vol.2(1) pp.037 - 048 November 2012
Available online http://www.globalresearchjournals.org/?a=journal&id=jcms

Full Length Research.

CORROSION RESISTANCE OF TYPE 444 FERRITIC STAINLESS STEEL IN ACIDIC CHLORIDE MEDIA

J.H. Potgieter[1], F.V. Adams[1], N. Maledi[1], J. Van Der Merwe [1,2] and P. A. Olubambi[3]

[1.] School of Chemical and Metallurgical Engineering, University of the Witwatersrand, Private Bag 3, Wits, 2050, Johannesburg, South Africa.
[2.] NRF/DST Centre of Excellence in Strong Materials, University of the Witwatersrand, Private Bag 3,Wits, 2050, Johannesburg, South Africa.
[3.] Department of Chemical and Metallurgical Engineering, Tshwane University of Technology, Pretoria, South Africa.
Corresponding Authors E-mail: salojohope@yahoo.com

Accepted May 2012.

The pitting corrosion resistance of the alloy 444 was studied by means of immersion tests and electrochemical techniques, including cyclic potentiodynamic polarization, open circuit corrosion potential measurements and chronoamperometry. All the corrosion measurements were carried out at room temperature and at varying concentrations of the electrolytes. The alloys were also characterized prior and after corrosion tests using a scanning electron microscope, and the corroded or passivated surfaces with a Raman spectrometer. The alloy displayed similar corrosion behaviour with slight differences in their corrosion resistance in all the solutions. The passivity of the alloy remained stable with none/little breakdown and pitting in 0.1 M of all the investigated solutions. Alloy 444 was better corrosion resistant in chloride environments than in the sulphuric acid. This was corroborated by SEM analysis, and 444 had more corrosion pits in sulphuric acid than in the chloride environments investigated.

Key words: *Ferritic stainless steel, acidic chloride media, corrosion resistance, mass loss tests, Raman spectra*

1.0 INTRODUCTION

The type 444 is a low-carbon, low nitrogen, ferritic stainless steel that provides pitting and crevice corrosion resistance superior to most ferritic stainless steels. Every application requiring superior corrosion resistance and resistance to chloride stress corrosion cracking is ideal for this alloy. Its current uses include food processing, brewery and wine-making equipment; hot-water tanks, heat exchanger tubing and automotive components. The type 444 ferritic stainless steel has received attention as a potential material for use in medicine, because it does not contain much nickel (Chiba *et al*., 1997).

It is well known that the addition of molybdenum (Mo) and small amounts of titanium (Ti) and/or niobium (Nb), to stainless steels contributes substantially to improve pitting corrosion resistance in aggressive chloride solutions (Clayton and Lu, 1986; Habazaki *et al*., 1991; Olsson, 1995; Qvarfort, 1998; Abdel *et al*., 2006; Van Warmelo *et al*., 2007). Corrosion studies on a welded 444 stainless steel demonstrated that dual stabilization with low individual concentrations of titanium and niobium may possibly provide optimum corrosion resistance (Dowling *et al.,* 1999).

The corrosion behaviour of Type 444 ferritic stainless steel has been described by a number of previous investigators. Schweitzer (2006) found that 444 ferritic stainless steel was resistant to very dilute H_2SO_4 at boiling temperature, but corroded rapidly at higher acid concentrations. According to Sekine *et al.* (1991), corrosion of Type 444 ferritic stainless steel would not be severe in aqueous acetic acid solution because the passivity of stainless steel is better in aqueous acetic acid solution than that of grades 410L, 430, 434, and XM27. Davies (1983) conducted a study on the effect of vanadium and other elements on the mechanical properties and corrosion resistance of ferritic stainless steels, including Type 444 in H_2SO_4, $FeCl_3$ and NaCl, and concluded that vanadium additions had several beneficial effects on the mechanical properties, as well as corrosion resistance of the investigated alloys. Asami and Hashimoto (2003) investigated the atmospheric corrosion resistance of various stainless steels, among them Type 444, and found it to be more corrosion resistant than other ferritic grades.

Sekine *et al.,* (1987, 1990) and Sekine and Okano(1989), studied the corrosion behaviour of ferritic stainless steels

Types 430, 410L, 434, and 444 in a number of organic acid media, including formic acid, oxalic acid and acetic acid, at various temperatures and concentrations. In all cases, Type 444 outperformed the other ferritic stainless steel grades. However, to date no record could be found that focused solely on the corrosion behaviour of Type 444 ferritic stainless steel in acidic chloride media and no specific industrial application of this alloy in acidic chloride media has been recorded. Since real industrial systems consists a mixture of both organic and minerals acids/salts, the investigations on the combined effect of chloride ions with mineral acids reported in this study typifies industrial conditions. The study thus provides material selection basis for the application of alloy 444 in industrial systems where acidic chloride solutions can be encountered. In the process the passive film formed under passivating conditions was also characterized to try and deduce the reason(s) for the observed corrosion behaviour.

2.0 MATERIALS AND METHODS

2.1 Materials

The ferritic stainless steel used in this investigation was type 444. Its chemical composition was determined by XRF spectrometry and ICP measurements and it is shown in Table 1.

Table 1: Chemical composition of 444 ferritic stainless steels

Elements	Compositions (mass %)
	444
C	0.012
S	0.006
P	0.022
Mn	0.450
Si	0.340
Ni	0.150
Cr	17.95
Mo	1.906
Ti	0.093
N	0.017
Co	0.020
Cu	0.090
B	NIL
Fe	balance

2.2 Reagents

The following pure and analytical grade reagents purchased from Merck Chemical, Johannesburg were used: Sulphuric acid (98 vol% H_2SO_4), Hydrochloric acid (37 vol %) and Sodium chloride. 0.1 M sulphuric acid, 0.1 M hydrochloric acid and 3.5 % sodium chloride were prepared from these pure and analytical grade reagents.

2.3 Materials characterization

As-received alloys for microstructural and morphological examination were prepared by cutting samples into squares of 1.5 cm, and these were hot mounted in bakelite. After mounting, the samples were mechanically ground successively on 240, 320, and 600 to 1000 grade silicon carbide papers. They were further polished using 1 to 6µm grades of diamond pastes to obtain a mirror-like surface. The surfaces were rinsed in distilled water and degreased with acetone. The degreased alloys were electro-etched with 10 % oxalic acid for about 5s to reveal the details of their microstructures for microstructural examination. Scanning electron microscopy (SEM) (model JEOL 840) was used in the microstructural study of the alloys after they were carbon coated in order to make their surface conductive. A Phillips (XL30 SERIES) SEM equipped with a field emission gun operating between 5 and 30 kV was used for analysis of selected points of interest. Raman spectroscopy (SENTERRA micro-Raman microscope) was used to investigate the surface composition of the alloys. The as-received alloys were characterised before immersion in the corrosive solutions. The Raman spectrometer was calibrated using a silicon wafer. Using a 50X objective and the 532 nm laser, sample spot sizes in the order of 4 -5 µm could be analysed. Using density

filters the laser power at the sample could be varied and in general the laser power delivered at the sample was 5 mW, with acquisition times typically at 10s. Spectra were recorded in the 50-1550 cm^{-1} spectral range. The OPUS^{TM} software package was used for data acquisition and analysis.

2.4 Corrosion studies

2.4.1 Weight loss tests

The samples for weight loss tests were prepared in accordance to the procedure recommended by ASTM G 1. The samples were cut to rectangular size of 2.5 cm by 1.5 cm with cross-sectional area of 0.45 cm^2. A hole of 5 mm diameter was drilled at one end of the samples, in which a string was attached for hanging them in the electrolytes. Before attaching strings to the samples, the samples were mechanically abraded with a series of emery papers up to 1000 grade. They were rinsed in acetone and distilled water to remove dirt, oils, and possible product formed on the surface of the samples.Polished and pre-weighed samples attached to strings were exposed to 0.1 M sulphuric acid, sulphuric acid containing 3.5 % NaCl solution and 0.1 M hydrochloric acid at room temperature. The weight loss experiment lasted for 92 days and weight losses measurements were carried out at four day intervals. The corrosion rate was calculated in micrometers per year. In each case duplicate experiments were conducted and the results varied within accepted experiment error. The electrolytes were changed before continuing with the subsequent tests. The mathematical formula by He (2002) was used to calculate the corrosion rates of the samples, namely:

$R_{corr} = 10^4$ ML/ (ρ.A.t)

Where R_{corr} **=** μm/y

ML = mass loss, g

A= exposed surface area of specimen, cm^2

t = time of exposure, yr

ρ = density of specimen, g/cm^3

2.4.2 Electrochemical studies

The electrochemical corrosion behaviour of the alloys was measured using a cyclic potentiodynamic scan, open circuit corrosion potential measurements and employing the chronoamperometry technique. Electrochemical measurements were done using an Autolab potentiostat (PGSTAT30 computer controlled) with the General Purpose Electrochemical Software (GPES) package version 4.9. All the measurements were made at room temperature using 0.1 M sulphuric acid, 0.1 M hydrochloric acid and 0.1 M sulphuric acid containing 3.5% NaCl. The alloys used for this investigation were cut similar to the samples for microstructural investigations, as described in section 2.3. They were prepared by attaching an insulated copper wire to one of their faces using an aluminum conducting tape, and cold mounted in epoxy resin. The alloys were abraded through 1000-grit silicon carbide metallurgical paper in accordance to ASTM-G59-97, degreased in acetone, and rinsed with distilled water.

Cyclic polarization measurements were carried out to determine the corrosion rates, evaluate the passivation behaviour, and to determine the potential pitting behaviour of the alloys. Before potentiodynamic polarization, the alloys were immersed in the electrolytes for 60 min to stabilize at the OCP. Cyclic polarization curves were measured at a scan rate of 0.2 mV/s starting from -250mV (with respect to the OCP) up to 1200mV. The variations in the open circuit potential values of the alloys were measured at zero applied current immediately after the immersion of the alloys in different media for up to about two hours. The chronoamperometric behaviour of the alloys was studied for eight hours in different media under an applied potential within the passivity regions, as obtained from the cyclic potentiodynamic polarization measurements in order to study the passive film/corrosion product on the surface of the alloy.

The conventional three electrode electrochemical cell system was used. The electrochemical cell was made of a 500 ml Pyrex glass conical flask suitable for the conventional three-electrode system. The cover of the cell had five holes for the reference electrode, working electrode, counter electrode, temperature measurement and aeration/de-aeration. The stainless steel samples were used as the working electrode, graphite rods as the counter electrodes and a silver/silver chloride 3 M KCl electrode as the reference electrode (SSE). Solutions were replaced after each test run and alloys were repolished for the subsequent scans to remove any possible corrosion product that might have formed on the surface of the alloy during the scanning. All the potentials reported were versus the SSE potentials.

3.0 RESULTS

3.1 CORROSION STUDIES

3.1.1 Weight loss tests

Corrosion behaviour of the alloy was studied using weight loss measurements in 0.1 M solutions of sulphuric acid, 0.1 M hydrochloric acid and in 0.1 M sulphuric acid containing 3.5% sodium chloride for 92 days. It was observed that when the alloy was immersed in the 0.1 M concentration of all the solutions used, the solutions turned to a dark green colour. Figures 1 and 2 show the corrosion rate (kinetic) curves of type 444 ferritic stainless steel after its exposure to 0.1 M sulphuric acid solution, 0.1 M hydrochloric acid, and 0.1 M sulphuric acid that contained 3.5 % NaCl solution for 92 days. The patterns observed for the cumulative weight loss versus immersion time for the alloy in all the solutions were closely related. There was a noticeable (about 8% for sulphuric acid, 3% for hydrochloric acid and 7% for sulphuric acid containing 3.5 % NaCl solution) increase in

the weight loss of the alloy in the first cycle of the test but no significant change was observed afterwards up unto the end of the test. Alloy 444 displayed the highest weight loss in the sulphuric acid solution. It was observed that the corrosion rates of the alloy in all the solutions initially increased followed by a steady decrease with an increase in immersion time.

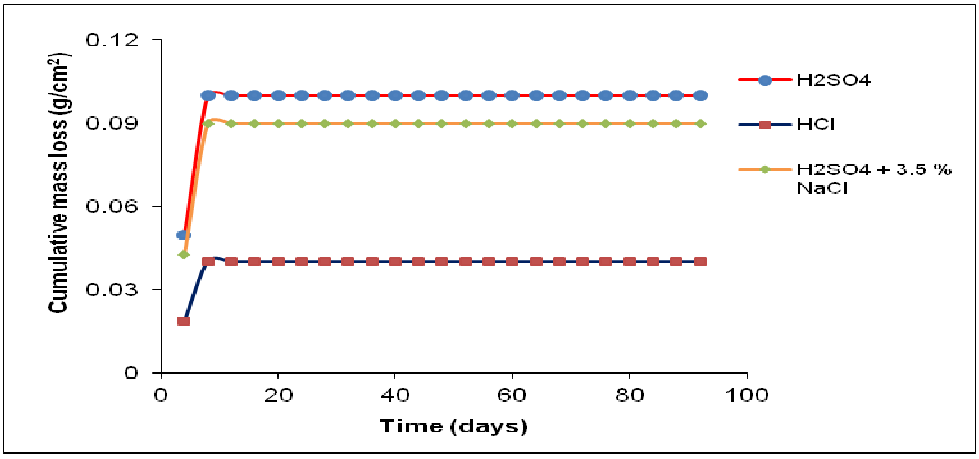

Figure 1: Cumulative weight loss of alloy 444 in 0.1 M of all the test solutions.

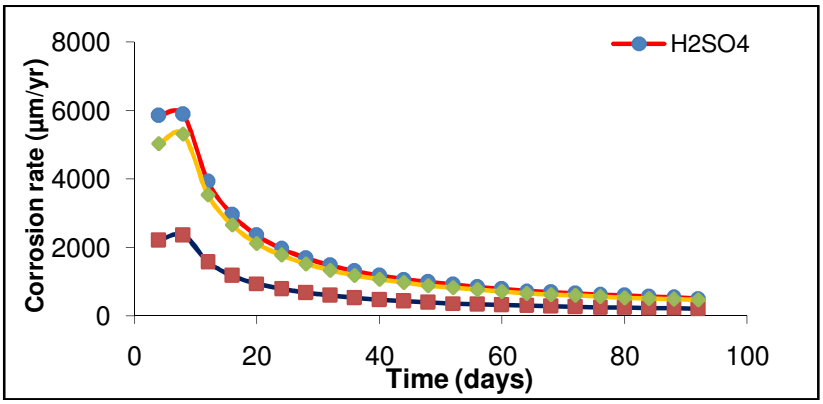

Figure 2: Corrosion rates of alloy 444 in 0.1 M of all the solutions.

A difference of 150 µm/yr was noticed in the corrosion rates values between the sulphuric acid solution and the sulphuric acid containing 3.5 % NaCl solution, with sulphuric acid solution causing the highest corrosion rate in the alloy. It was observed that alloy 444 generally exhibited higher corrosion resistance in hydrochloric acid compared to sulphuric acid solutions. The corrosion rate of 444 in hydrochloric acid was one order of magnitude lower than in sulphuric acid and sulphuric acid containing 3.5% NaCl. Table 2 shows the corrosion rates obtained from weight loss tests of the alloy in 0.1 M concentrations of all the solutions within an experimental error of ± 0.5 x 10^3. The corrosion rate of alloy 444 seems to increase in the order hydrochloric acid < sulphuric acid containing 3.5 % NaCl < sulphuric acid.

Table 2: Summary of the corrosion rates of alloy 444 in 0.1 M of all the solutions for 92 days.

Media	Corrosion rate (µm/yr)
H_2SO_4	1.65 x10^3
HCl	6.60 x 10^2
H_2SO_4 + 3.5 % NaCl	1.50 x 10^3

3.1.2 Open circuit potential variations with time

A study on the reactivity of the alloys, i.e. their tendencies to corrode in the different media with time, was carried out using Open Circuit Potential (OCP) measurements. The variations in the OCP values of the alloys were studied at zero applied current immediately after the immersion of the alloys in the different media for two hours. The variation in open-circuit potential as a function of time for alloy 444 tested in 0.1 M sulphuric acid, 0.1 M hydrochloric acid, and 0.1 M sulphuric acid containing 3.5 % NaCl solutions are presented in Figure 3. The potential was observed to generally shift toward more positive values with time. This trend is very slight in the case of the two sulphuric acid solutions. In 0.1 M hydrochloric acid, there was a small and progressive increase in the potential of the alloy right from the onset, while potential values in sulphuric acid and sulphuric acid containing 3.5 % NaCl solution decreased initially before increasing. No significant difference was observed in the OCP curves of the alloy in 0.1 M sulphuric acid and in sulphuric acid containing 3.5 % NaCl solution.

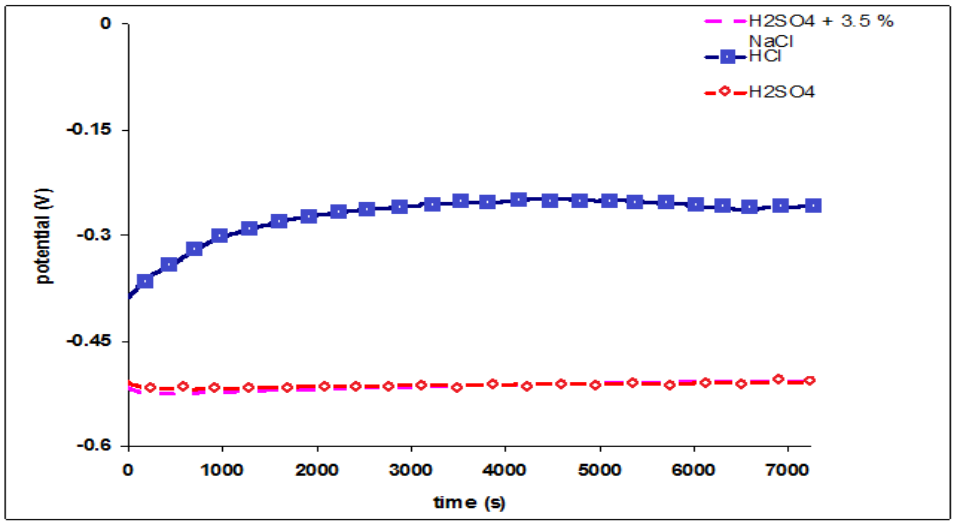

Figure 3: Open circuit potential of alloy 444 in 0.1 M of all the solutions

3.1.3 Potentiodynamic tests

The electrochemical data obtained from the potentiodynamic polarization scans in 0.1 M of all the solutions are summarized in Table 3. In the solutions investigated, alloy 444 displayed a more noble corrosion potential in hydrochloric acid than in sulphuric acid containing 3.5 % NaCl and sulphuric acid similar to the initial observation from the weight loss test. The critical current densities of the alloy in 0.1 M sulphuric acid and sulphuric acid containing 3.5 % NaCl are of the same order of magnitude, while that of the alloy in 0.1 M hydrochloric acid was substantially lower in comparison. The passive current density of alloy 444 was similar in all three solutions investigated. The corrosion current density was lower in 0.1 M hydrochloric acid compared to the other two solutions

Table 3: Corrosion data obtained from cyclic potentiodynamic curves of alloy 444 in 0.1 M of all the solutions.

Corrosion media	E_{corr} (V)	i_{corr}(A/cm^2) x 10^{-5}	i_{crit}(A/cm^2) x 10^{-3}	$i_{passive}$(A/cm^2) x 10^{-4}	Corrosion Rate (mm/yr) X10^{-1}
0.1M H_2SO_4	-0.512	2.7	2.4	3.1	3.0
0.1M H_2SO_4 + Cl^-	-0.516	1.3	1.5	1.1	1.4
0.1M HCl	-0.428	0.14	0.53	7.1	0.16

3.1.4 Chronoamperometric tests

Chronoamperometric behavior was studied for about eight hours in different media at an applied potential of 0.6 V, which was within the passivity region. Figure 5 shows the chronoamperometry curves of alloy 444 in 0.1 M of all the solutions. The results showed that the passive currents of the alloy decreased with time before stabilizing mostly for samples in sulphuric acid solution and hydrochloric acid. However, the initial decrease in the passive current of the alloy in sulphuric acid containing 3.5 % NaCl steadily increased before stabilizing. The result also showed that the passive film seems to be more stable in hydrochloric acid than in sulphuric acid containing 3.5 % NaCl and sulphuric acid alone, as the current density did not show a distinct increase before stabilizing. The passive film formed during polarisation was therefore not immediately stable and well established.

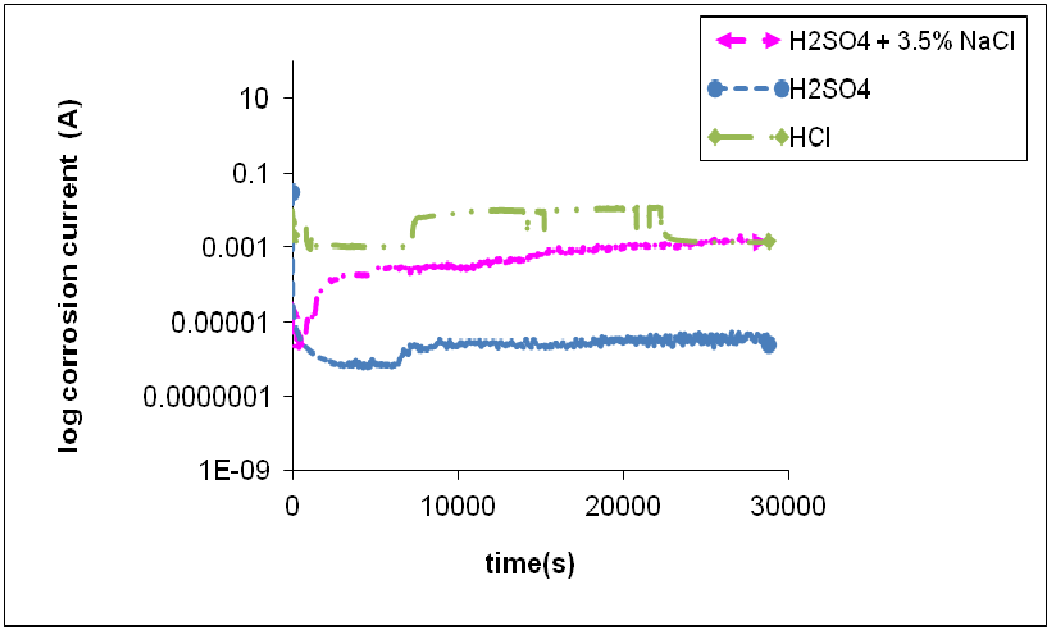

Figure 5: Chronoamperometry curves of alloy 444 in 0.1 M of all the solutions at 0.6V.

3.2 ANALYSIS OF SURFACE CORROSION PRODUCTS

3.2.1 Analysis of surface corrosion products of alloy 444 after exposure to corrosive solutions (0.1 M hydrochloric acid, 0.1 M sulphuric acid and 0.1 M sulphuric acid containing 3.5 % NaCl solution)

The Raman spectra in Figure 6 detected compounds of iron, nickel and molybdenum on the surface of the alloy after exposure to the corrosive solutions. A titanium compound was also encountered at two band widths. The observed shifts were very similar to the observations which were reported earlier by Hart *et al.,*(1976); Gui and Devine (1991); Vuurman and Wachs (1992); Chang *et al.* (1992); and Guevara-Lara *et al.,* (2007).

3.2.2 Effect of chloride on the surface corrosion products of alloy 444

The Raman spectra of alloy 444 after corrosion in sulphuric acid containing 3.5 % NaCl is shown in Figure 6c and Raman bands were observed at 275, 398 and 615 cm^{-1}. In 0.1 M hydrochloric acid (Figure 6d) three shifts were observed at 217, 299 and 392 cm^{-1}. These could correspond to α–Fe_2O_3 and TiO_2. Molybdenum compounds were not observed on this spectrum compared to the spectra of the alloy after corrosion in sulphuric acid and sulphuric acid containing 3.5 % NaCl solution. The Raman spectroscopy results are further discussed in section 4.2.

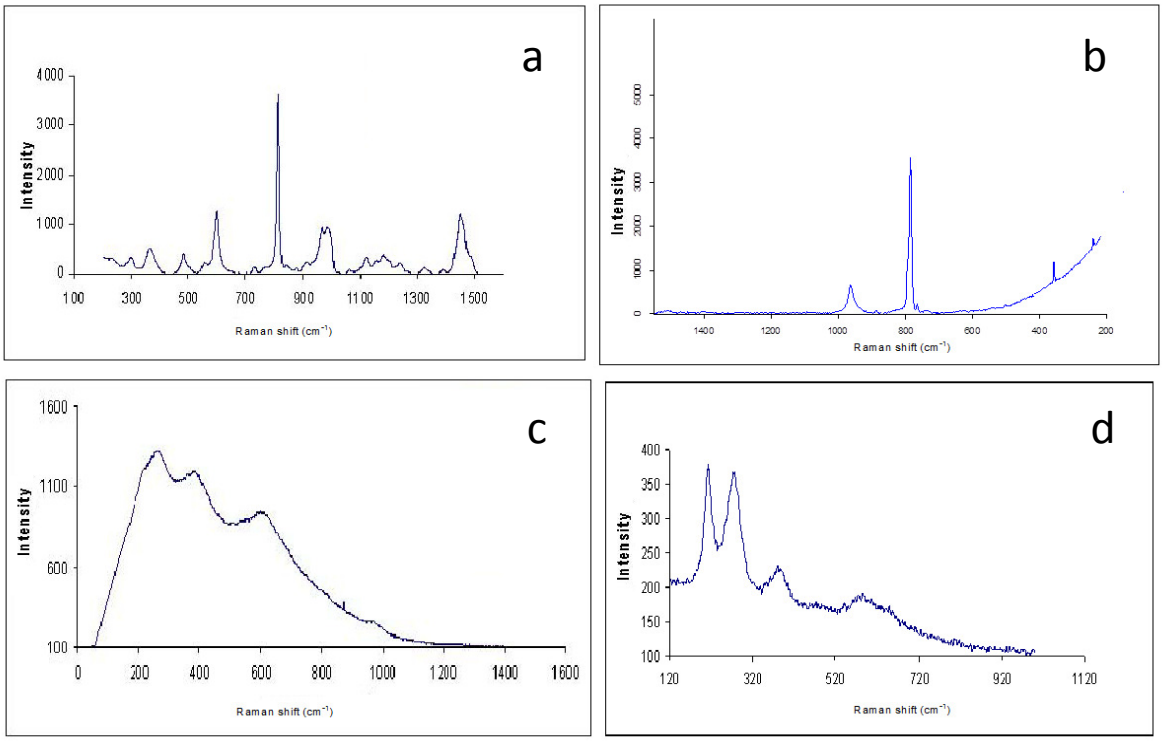

Figure 6: Raman spectrum of (a) as-received alloy 444 (b) after corrosion in 0.1 M sulphuric acid (c) after corrosion in 0.1 M sulphuric acid containing 3.5 % NaCl (d) after corrosion in 0.1 M HCl.

3.2.3 Morphological studies

The micrographs obtained from the SEM analysis of the as-received sample electro-etched in oxalic acid, after corrosion in 0.1 M sulphuric acid, 0.1 M sulphuric acid containing 3.5 % NaCl solution and 0.1 M HCl are shown in Figure 7. The micrographs showed more details of the grain size and structure of the alloys. There was no noticeable pit on the SEM micrographs of alloy 444 obtained after corrosion in all the solutions. This implies formation of passive films on the surface of the alloy after exposure to all the solutions. This finding confirmed the result from the corrosion rates of the alloy in all the solutions.

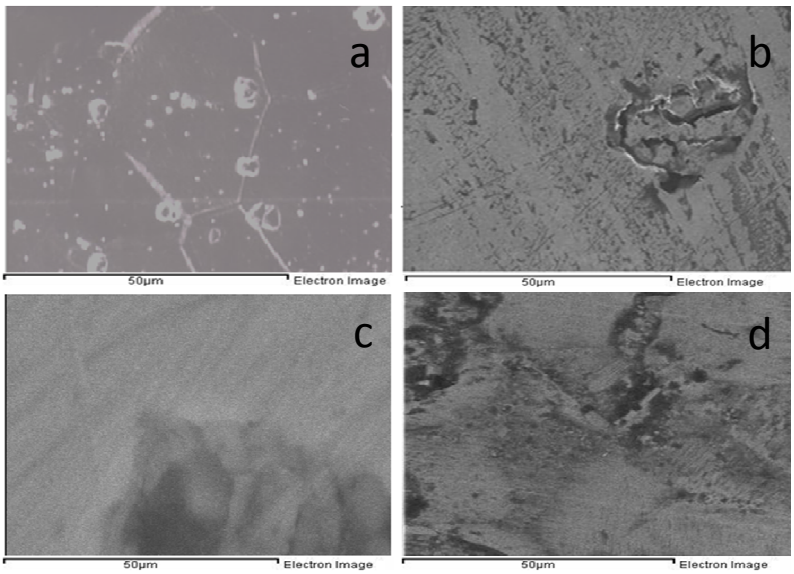

Figure 7: Secondary electron micrograph showing the morphology 444 (b) after corrosion in 0.1 M hydrochloric acid (c) after corrosion in 0.1 M sulphuric acid containing 3.5 % NaCl (d) after corrosion in 0.1 M sulphuric of (a) as-received alloy acid.

4.0 DISCUSSION

4.1 CORROSION STUDIES

4.1.1 Weight loss tests

The observed change in the solution colour during the weight loss tests was similar to the observations made by Pardo *et al.*,(2008) when carrying out an investigation on the influence of manganese and molybdenum additions on corrosion resistance of AISI 304 and 316 stainless steels in 30 wt. % H_2SO_4 at 25 and 50 ^{0}C. These authors observed that when the specimen gets in contact with the sulphuric acid medium, the passive layers of the AISI 304 and AISI 316 completely dissolved and the solution turns to a dark green colour typical of the Cr (III) species. AISI 316 stainless steel has an essential ability to form a protective oxide or "passive" layer on its surface. This protective layer is thought to consist of a heterogeneous chromium oxide film (Cr_2O_3) along with elemental iron, nickel, and their respective oxides. In general, this passive layer protects the steel from oxidation. However, when subjected to extremely corrosive environments, the heterogeneous film is attacked and chemical reduction occurs. When the oxide film layer is dissolved beyond regeneration, localized corrosion takes place in the bulk alloy and reaction by-products are generated. There was a noticeable increase in the weight loss of the alloy in the first cycle of the test but no significant change was observed afterwards up unto the end of the test. This suggested that there was a breakdown in the film on the surface of alloy 444 in the initial stages, followed by the formation of a new passive film after dissolution. This may also indicate that the alloy was in the passive state throughout the rest of the test. The presence of titanium coupled with molybdenum could add to the stability of film formed in alloy 444. Dowling *et al.,* (1999) reported that dual stabilization of a welded 444 stainless steel with titanium and niobium may possibly provide optimum corrosion resistance. In general, the corrosiveness of acids increases as the size of the acid molecule decreases. Differences in corrosion inhibition in different media cannot only be attributed to differences in K_a (acid strength), but also to knowledge of buffer capacity, ionic strength, conductivity, molecular sizes, complex formation by the conjugated base anions, as well as various corrosion process conditions.

Eventually there was no substantial difference in the corrosion rates values between the SO_4^{2-} and Cl^- media. This may possibly be due to the insignificant difference in the extent of change of the oxide film on the steel surface by the electrolyte species. Pitting corrosion is triggered by the susceptible spots formed on the surface of a metal. As a pit forms, the metal goes into solution and increases the flow of current. As the number of the active spots on the surface increases, the probability of the stable pits formation also increases (Shahryari *et al.*, 2008).It was observed that alloy 444 generally exhibited slightly higher corrosion resistance in hydrochloric acid compared to sulphuric acid solution. Similar observations were made by Ameer *et al.* (2004), who showed that the corrosion rate of the alloy tested was higher in the sulphate medium as compared with the chloride solution at comparable concentration. Betova *et al.,* (2002) also reported that the rate of transpassive dissolution of highly alloyed stainless steels is the lowest in chloride solutions and the highest in sulphate electrolytes. According to Olefjord and Fischmeister (1975), the chloride ions can be incorporated into the passive film when a Mo-containing stainless steel was exposed in hydrochloric acid at various potentials in the active and passive ranges of the alloys. It is suggested that molybdenum can form strong soluble oxochlorocomplexes, which decrease the free Cl^- ion concentration close to surface during passivation. The presence of an adequate amount of chromium is also indispensable for the improvement of pitting resistance (Sugimoto and Sawada, 1976).

4.1.2 Open circuit potential variations with time

In 0.1 M hydrochloric acid, there was a small and progressive increase in the potential of the alloy right from the onset, while potential values in sulphuric acid and sulphuric acid containing 3.5 % NaCl solution decreased initially before increasing slightly. This suggested that there was same breakdown in the film on the surface of alloy 444 during the initial stages, followed by the formation of a new passive film after dissolution. This correlated with the observed weight loss test results.

4.1.3 Potentiodynamic tests

Figure 4a gives a graphical representation of the responses to polarization. It is observed that the alloy display distinct and typical active to passive transition behavior during polarization from active to more noble potentials. It was observed that alloy 444 generally exhibited higher corrosion resistance in chloride media compared to sulphate media, and this is in agreement with the results from the weight loss tests. It was observed that chloride additions caused a small increase in the passive current density (i_{pass}) of the acid media, as well as a slight lowering in i_{crit} and i_{corr}. Similar results were found by Bojinov *et al.*, (2001) in studies of the electrochemical behaviour of anodic films on pure Cr, Fe–Cr alloys and Fe–Cr–Mo alloys in 1 M sulphuric acid solution.

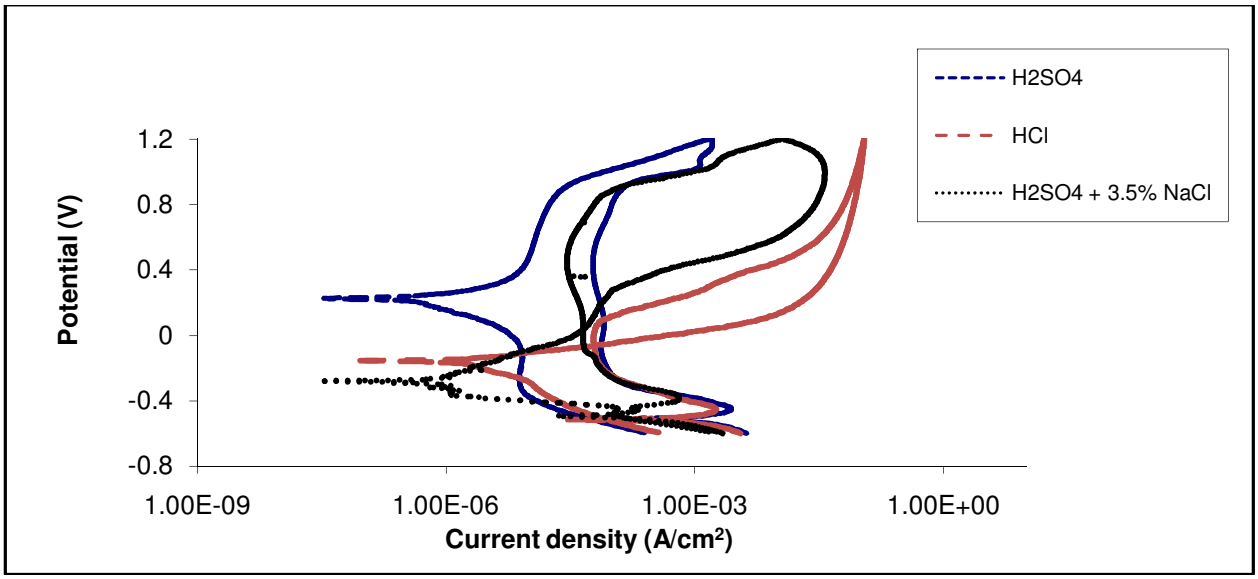

Figure 4a: Cyclic potentiodynamic polarisation curve of alloy 444 in 0.1 M of all the solutions

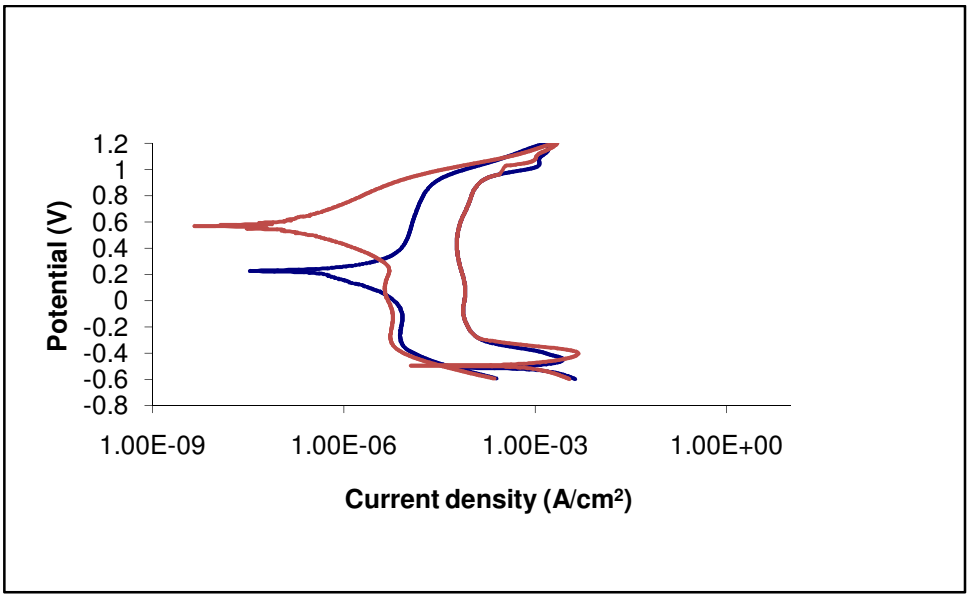

Figure 4b: Cyclic potentiodynamic polarisation reproducibility curve of alloy 444 in 0.1 M sulphuric acid solution

4.1.4 Chronoamperometric tests

Chronoamperometric tests were carried out to further assess the potential pitting corrosion behaviour of the alloy, and to determine the stability of passive films formed in the different media. The results (Fig. 5) showed that the passive currents of the alloy in single media acid solutions decreased with time before stabilizing. This is in agreement with the results reported by Shahryari *et al.* (2008). The pitting potential region could result in the formation of pits on the alloys' surfaces, followed by their repassivation, and this is manifested as a series of sharp current spikes. The propagation (growth) of the pit to form a critical-pit was not thermodynamically and kinetically favourable, so the pit eventually repassivates and consequently the current stabilizes with time to yield the latter smooth parts observed in each curve. It was observed that alloy 444 generally exhibited slightly better corrosion resistance in hydrochloric acid compared to sulphuric acid solution. The chloride ions can be incorporated into the passive film when a Mo-containing stainless steel was exposed in hydrochloric acid at various potentials in the active and passive ranges of the alloys. Molybdenum can form strong soluble oxochloro-complexes, which thereby will decrease the free Cl^- ion concentration close to surface during passivation. Also,

the presence of titanium in alloy 444 favours chloride environment compared to sulphuric acid.

4.2 ANALYSIS OF SURFACE CORROSION PRODUCTS

4.2.1 Analysis of surface corrosion products of alloy 444 after corrosion in 0.1 M sulphuric acid solution

The shifts observed for alloy 444 in the Raman spectra (Fig. 6b), two were quite prominent, namely those at 963 and 766.1 cm^{-1} (Table 4). These shifts correspond to MoO_3 and NiO respectively (Maledi, 2007). Two minor bands occurred at 357 cm^{-1} ($Mo_7O_{24}^{6-}$) and 240 cm^{-1} (α-Fe_2O_3). MoO_3 was formed on the surface of the alloy after corrosion in sulphuric acid, and sulphuric acid containing 3.5 % NaCl. These were obtained at 963 and 275 cm^{-1} respectively. There were no compounds of chromium detected after corrosion in 0.1 M sulphuric acid, which could mean there was active dissolution of chromium into all the solutions. This would explain the colour change in the solutions during the corrosion test.

Table 4: Summary of the Raman spectrum of the corrosion products formed on alloy 444 tested in 0.1 M sulphuric acid, 0.1 M sulphuric acid containing 3.5 % NaCl and 0.1 M HCl

Media	Raman shift (cm^{-1}) from this study	References (cm^{-1})	Probable corrosion product/compound
H_2SO_4	963	960	MoO_3
	766.1	760	NiO
	766.2	760	NiO
	357	350	$Mo_7O_{24}^{6-}$
H_2SO_4 + 3.5 % NaCl	275	282	MoO_3
	398	398	TiO_2
	615	613	α-Fe_2O_3
HCl	217	220	α-Fe_2O_3
	299	299	α-Fe_2O_3
	392	398	TiO_2

4.2.2 Effect of chloride on the surface corrosion products of alloy 444

The corrosion products on the surface of the alloy after corrosion in hydrochloric acid contain α-Fe_2O_3 and TiO_2 with shifts observed at 217, 299 and 392 cm^{-1}. The results obtained imply that the addition of chloride did have a significant effect on the nature of the corrosion products obtained after corrosion. It was established that TiO_2 and α-Fe_2O_3 were only formed in chloride environment while molybdenum and nickel oxides were formed in solutions containing sulphate ions only. The observed products on the surface of the alloy confirmed earlier observations by Doh *et al.* (2003) as well as predictions by Clayton and Lu (1986), Habazaki *et al.* (1991), Olsson (1995), Qvarfort (1998), Abdel *et al.* (2006) and Van Warmelo *et al.* (2007) on the role of molybdenum and titanium in the formation of passive films and improving corrosion resistance.

4.3 MORPHOLOGICAL STUDIES

Chromium, molybdenum and nitrogen are the alloying elements that could increase the resistance of stainless steels to both pitting and crevice corrosion. In a chloride environment, nickel could form a stable passive nickel oxide layer (Jiangzhou and Wang, 2001; Singh and Singh, 2002; Abd El Aal, 2003 and Munoz *et al.*, 2006). By physical observation, more noticeable pits were observed on the surfaces of the alloys in sulphuric acid solution compared to when chloride ion was added to sulphuric acid, which is contrary to conventional wisdom and expectations. However, Ameer *et al.* (2004) also found that the corrosion rate of the alloys tested in the sulphate medium was higher compared with the chloride solution at comparable concentration. Betova *et al.* (2002) also reported that the rate of transpassive

dissolution of highly alloyed stainless steels is the lowest in chloride solutions and the highest in sulphate containing media.

CONCLUSIONS

The alloy differs in its corrosion resistance in all the solutions. It was more corrosion resistant in chloride environments (hydrochloric acid and sulphuric acid containing 3.5 % NaCl) than in the sulphuric acid in both types of tests conducted. SEM analysis showed that alloy 444 formed more corrosion pits in sulphuric acid than in chloride environments. This corroborated the different resistances of the alloy in both sulphate and chloride environments as obtained from the electrochemical investigation and weight loss tests. The presence of compounds of titanium as observed in the Raman spectra of the corrosion products of alloy 444 in chloride environments could be responsible for the good corrosion resistance of alloy 444 in chloride environments. The presence of titanium and molybdenum oxides confirms work and predictions by other earlier workers recorded in the literature. NiO as a component of the passive film was only detected after exposure to sulphuric acid, while TiO_2 as a component of the passive film only appears when Cl^- ions were present in the corrosive environment. Because the passive film seems to be more stable in acidic chloride (containing) solutions than in sulphuric acid, one can conclude that the alloy is suitable for use in chloride environments. If it has to be used in sulphuric acid, its conductivity (sulphuric acid) has to be taken into consideration.

ACKNOWLEDGEMENTS

The authors thank the South African Stainless Steel Development Association (SASSDA) for the supply of the material used in this investigation, and the University of the Witwatersrand (Wits) for the use of laboratory facilities and equipment.

REFERENCES

Abd El Aal, E. E. (2003). Breakdown of passive film on nickel in borate solutions containing halide anions. *Corrosion Science,* 45, pp. 759-775.

Abdel, S. H., Eman, E-S. and El-Bitar, T. (2006).The corrosion behavior of niobium bearing cold deformed austenitic stainless steels in 3.5% NaCl. *Materials Letters*, 61, pp. 2827-2832.

Ameer, M.A., Fekry, A.M. and Heakal, F. E-T. (2004). Electrochemical behaviour of passive films on molybdenum-containing austenitic stainless steels in aqueous solutions. *Electrochimica Acta,* 50, pp. 43-49.

Asami, K. and Hashimoto, K. (2003). Importance of initial surface film in the degradation of stainless steels by atmospheric exposure. *Corrosion Science*, 45, pp. 2263–2283.

Betova, I., Bojinov, M., Laitinen, T., Makela, K., Pohjanne, P. and Saario, T. (2002). The transpassive dissolution mechanism of highly alloyed stainless steels I. Experimental results and modelling procedure. *Corrosion Science,* 44, pp. 2675-2697.

Bojinov, M., Fabricius, G., Laitinen, T., Makela, K., Saario, T. and Sundholm, G. (2001). Influence of molybdenum on the conduction mechanism in passive films on Iron–Chromium alloys in sulphuric acid solution, *Electrochimica Acta,* 46, pp. 1339–1358.

Chang, S.C., Leugers, M.A. and Bare, S.R. (1992). Surface Chemistry of Magnesium Oxide-Supported Molybdenum Oxide: An In-situ Raman spectroscopic study. *Physical Chemistry,* 96, pp. 10358-10365.

Chiba, A., Sakakura, S., Kobayashi, K. and Kusayanagi, K. (1997). Dissolution amounts of nickel, chromium and iron from SUS 304, 316 and 444 stainless steels in sodium chloride solutions, *Materials Science,* 32, pp. 1995-2000.

Clayton, C.R., and Lu, Y.C. (1986). A bipolar model of the passivity of stainless steel: The role of Mo addition. *Journal of the Electrochemical Society*, 133, pp. 2465–2473.

Davies, R.D. (1983). The effect of vanadium and other elements on the mechanical properties and corrosion resistance of ferritic stainless steels. MSc. Dissertation, University of the Witwatersrand.

Doh, S. J., Je J. H., Kim, J. S., Kim, K. Y., Kim, H. S., Lee, Y. D., Lee, J. M. and Hwu, Y. (2003). Influence of Cr and Mo on the passivation of stainless steel 430 (18Cr) and 444 (18Cr–2Mo): In situ XANES study. *Nuclear Instruments and Methods in Physics Research B,* 199, pp. 211–215.

Dowling, N.J.E., Kim, Y.-H., Ahn, S.-K. and Lee, Y.-D. (1999). Effect of alloying elements and residuals on corrosion resistance of type 444 stainless steel. *Corrosion Science*, 55, pp. 187-199.

Guevara-Lara, A., Bacaud, R. and Vrinat, M. (2007). Highly active $NiMo/TiO_2–Al_2O_3$ catalysts: Influence of the preparation and the activation conditions on the catalytic activity. *Applied Catalysis,* 328, pp. 99–108.

Gui, J. and Devine, T. M. (1991). In-situ vibrational spectra of the passive film on iron in buffered borate solution. *Corrosion Science,* 32, pp. 1105-1124.

Habazaki, H., Kawashima, A., Asami, K. and Hashimoto, K. (1991). The effect of molybdenum on the corrosion behavior of amorphous Fe-Cr-Mo-P-C alloys in hydrochloric acid. *Materials Science and Engineering,* 13, pp. 1033-1036.

Hart, T. R., Adams, S. B and Tempkin, H. (1976). Light scattering in solids (Edited by M. Balkanski, R. L. and S. Porto). Flammarion Sciences, Paris, pp 254-259.

He, W. (2002). Atmospheric corrosion and runoff processes on copper and zinc as roofing materials. Doctoral Thesis, Department of Materials Science and Engineering, Division of Corrosion Science, Royal Institute of Technology, SE-10044, Stockholm, Sweden.

Jiangzhou, S. and Wang, R. Z. (2001). Experimental research on characteristics of corrosion-resisting nickel alloy tube used in triple-effect $LiBr/H_2O$ absorption chiller. *Applied Thermal Engineering*, 21, pp. 1161–1173.

Maledi, N.B. (2007). Corrosion behaviour of Pt-based superalloys intended for high temperature applications. MSc. Dissertation, University of the Witwatersrand.

Munoz, A. I., Anton, J. G., Guinon, J. L. and Herranz, V. P. (2006). Effects of solution temperature on localized corrosion of high nickel content stainless steels and nickel in chromated LiBr solution. *Corrosion Science*, 48, pp. 3349–3374.

Olefjord, I. and Fischmeister, H. (1975). ESCA studies of the composition profile of low temperature oxide formed on chromium steels—II. Corrosion in oxygenated water. *Corrosion Science,* 15, pp. 697-707.

Olsson, C-O. A. (1995). The influence of nitrogen and molybdenum on passive films formed on the austenoferritic stainless steel 2205 studied by AES and XPS. *Corrosion Science*, 37, pp. 467-479.

Pardo, A., Merino, M.C., Coy, A.E., Viejo, F., Arrabal, R. and Matykina, E. (2008). Effect of Mo and Mn additions on the corrosion behavior of AISI 304 and 316 stainless steels in H_2SO_4. *Corrosion Science*, 50, pp. 780-794.

Qvarfort, R. (1998). Some observations regarding the influence of molybdenum on the pitting corrosion resistance of stainless steels. *Corrosion Science*, 40, pp. 215- 223.

Schweitzer, P.A. (2006). Fundamentals of metallic corrosion: Atmospheric and media corrosion of metals. Corrosion Engineering Handbook. CRC Press, New York, pp 128-132.

Sekine, I., Hatakeyama, S. and Nakazawa, Y. (1987). Effect of water content on the corrosion behavior of type 430 stainless steel in formic and acetic acids. *Electrochimica Acta,* 32, pp. 915-920.

Sekine, I., and Okano, C. (1989). Corrosion behaviour of mild steels and ferritic stainless steels in oxalic acid solutions. *Corrosion Science,* 45, pp. 924-932.

Sekine, I., Okano, C. and Yuasa, M. (1990). The corrosion behavior of ferritic Stainless steel in oxalic acid solutions. *Corrosion Science,* 30, pp. 351-366.

Sekine, I., Kawase, T., Kobayashi, M. and Yuasa, M. (1991). The effects of chromium and molybdenum on the corrosion behavior of ferritic stainless steels in boiling acetic acid solutions. *Corrosion Science,* 32, pp. 815-825.

Shahryari, A., Omanovic, S. and Szpunar, J.A. (2008). Electrochemical formation of highly pitting resistant passive films on a biomedical grade 316LVM stainless steel surface. *Materials Science and Engineering,* 28, pp. 94–106.

Singh, A. K. and Singh, G. (2002). Corrosion of stainless steels in chlorine dioxide solution. *Anti-Corrosion Methods and Materials*, 49, pp. 417–425.

Sugimoto, K. and Sawada, Y. (1976). Role of alloyed molybdenum in austenitic stainless steels in the inhibition of pitting in neutral halide solutions. *Corrosion Science,* 32, pp. 347–352.

Van Warmelo, M., Nolan, D. and Norrish, J. (2007). Mitigation of sensitization effects in unstabilised 12%Cr ferritic stainless steel welds. *Materials Science and Engineering,* 464, pp. 157-169.

Vuurman, M.A. and Wachs, I.E. (1992). In-situ Raman spectroscopy of alumina-supported metal oxide catalysts. *Physical Chemistry*, 96, pp. 5008-5016.